ISSN 0030-400X, Optics and Spectroscopy, 2010, Vol. 109, No. 2, pp. 197–204. © Pleiades Publishing, Ltd., 2010.
Original Russian Text © A.N. Bashkatov, E.A. Genina, V.I. Kochubey, V.V. Tuchin, 2010, published in Optika i Spektroskopiya, 2010, Vol. 109, No. 2, pp. 226–234.

BIOMEDICAL OPTICS AND SPECTROSCOPY

Optical Properties of Human Sclera in Spectral Range 370–2500 nm

A. N. Bashkatov, E. A. Genina, V. I. Kochubey, and V. V. Tuchin

Saratov State University, Saratov, 410012 Russia

e-mail: a.n.bashkatov@mail.ru

Received February 11, 2010

Abstract—Optical characteristics of human sclera are experimentally studied. Experiments are performed in vitro on a Cary-2415 spectrophotometer in the spectral range 370–2500 nm. Based on the measured diffuse reflection and total transmission spectra, the absorption and transport scattering coefficient spectra are calculated by the inverse adding–doubling method.

DOI: 10.1134/S0030400X10080084

INTRODUCTION

The knowledge of optical characteristics of biotissues is a key point in the development of mathematical models that adequately describe the propagation of light in biotissues. These models are fundamentally important for the development of new optical methods used in different fields of biology and medicine for the photodynamic and photothermal destruction of cells and tissues, as well as for the development of new approaches in optical tomography, optical biopsy, etc. [1–4]. However, despite the fact that the optical parameters of biotissues have been determined in numerous works, the optical properties of many biotissues in a wide wavelength range still remain unknown, although the analysis of the absorption of visible and near-IR radiation by biotissues is a matter of principle for the development of methods of optical diagnostics and photodynamic and photothermal therapy of various diseases. In addition, the behavior of scattering characteristics of biotissues in the range of absorption bands remains insufficiently studied. In particular, the deviation of the spectral dependence of scattering characteristics from the classical (monotonic) dependence is frequently attributed to calculation or experimental errors [5]. At the same time, in laser therapy, it is hardly possible to monitor optical radiation at all without taking into account scattering characteristics of biotissues. For this reason, the analysis of light scattering in the range of absorption bands is a very important problem in the optics of biotissues.

In ophthalmology, optical methods have been widely used in the diagnostics and therapy of glaucoma and the optical tomography of eyeground, as well as in studying tissue metabolism and pathological changes in eye tissues due to various diseases, etc. [2, 4, 6–9]. Knowledge of the optical characteristics of superficial fibrous tissues, in particular of the sclera, is of fundamental importance in this case for the development of new methods and the optimization of existing methods of optical tomography, coherent and confocal microscopy, increasing the informativity of reflection spectroscopy methods, dosimetry of laser transscleral coagulation of ciliary body, etc. However, despite the fact that these investigations are very important, at present, there still exists only a limited number of works [6–10] devoted to the study of optical characteristics of human sclera. The objective of this study is to determine scattering and absorption characteristics of human sclera in the spectral 370–2500 nm.

MATERIALS AND METHODS

As materials for study, we used ten samples of human sclera that were obtained as a result of elective eye-removal surgery operations. Immediately after biopsy, samples of sclera were placed in a 0.9% NaCl solution and, prior to performing spectral measurements, were stored in it within 2–3 h at a temperature about 20°C. The area of samples was in the range 300–400 mm^2. To measure the thickness of the samples, they were placed between two slides; the measurements were performed with a micrometer at several points of each sample. The accuracy of each measurement was ±50 μm. The obtained values were averaged. The thickness of the experimental samples was 1–2 mm and, on average, was 1.5 ± 0.5 mm. The optical properties were studied in the spectral range of 370–2500 nm on a Cary-2415 spectrophotometer (Varian, Australia) equipped with an integrating sphere. This instrument is a two-channel diffraction monochromator with an incorporated control and signal detection system. A halogen incandescent lamp was used as a radiation source. The size of a light beam incident on the sample was 5 × 5 mm. The scanning rate was 2 nm/s.

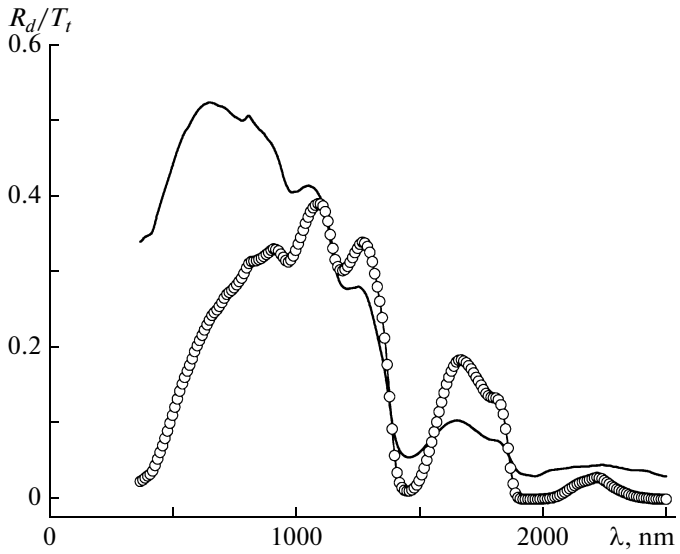

Fig. 1. Spectra of diffuse reflection (R_d) and total transmission (T_t) of sample of human sclera. Solid curve is diffuse reflection spectrum and symbols correspond to total transmission spectrum. Sample thickness is 1.0 ± 0.05 mm.

To process the experimental data and to determine the optical parameters of sclera, the inverse adding–doubling (IAD) method was used [11]. This method is widely applied in the optics of biotissues for the processing data of spectrophotometry obtained using integrating spheres [5, 6, 10, 12–20]. The IAD method makes it possible to determine the absorption coefficient μ_a and the transport scattering coefficient $\mu_s' = \mu_s(1-g)$ of a biotissue using the coefficients of the diffuse reflection and total transmission. Here, μ_s is the scattering coefficient and g is the scattering anisotropy factor. In calculations, the anisotropy factor was fixed to be 0.8, since this value is the most typical for the majority of biotissues in the visible and near-IR spectral ranges [4].

The IAD method is widely used to process the data of spectrophotometric measurements because this method does not depend on the ratio between the absorption and scattering coefficients of biotissues [11], which is its main advantage compared to other methods of solving the radiation transfer equation in strongly scattering media, e.g., compared to the diffusion approximation of the theory of radiation transfer [21–23] or the Kubelka–Munk method [24–26], which are rather frequently used in the optics of biotissues and require the implementation of the condition $\mu_a/\mu_s \ll 1$ [1–4] as a basic criterion of applicability. This feature of the IAD method becomes fundamentally important when optical characteristics of biotissues should be determined in the range of strong absorption bands where the absorption and scattering coefficients become comparable. The main limitation of the IAD method is related to possible losses of scattered radiation through side surfaces of the sample of the biotissue [27], which may be possible if the size of the sample is small compared to the size of the light beam incident on the biotissue sample or when the biotissue is characterized by comparatively small absorption and scattering coefficients. If side losses of probing radiation arise and they are not taken into account, the determined absorption coefficient proves to be overestimated [27]. For the application of the IAD method to be correct, it is necessary for the distance from the edge of the probing beam incident on the sample of biotissue to the nearest boundary of the sample to be greater than the photon transport mean free pathlength, which is defined as $1/(\mu_a + \mu_s')$ [1].

The optical parameters were calculated separately for each spectral point. The used algorithm includes the following steps:

(i) setting the initial values of μ_a and μ_s' using the analytical expressions for them presented in [19] with reference to [11];

(ii) calculating the diffuse reflection and total transmission coefficients by the adding–doubling method [28] using the initial values of μ_a and μ_s';

(iii) comparing the calculated and experimentally measured values of these coefficients;

(iv) performing the iterative procedure until the calculated and experimental data match each other within a specified accuracy.

As an iterative procedure, we used the Nelder–Mead simplex method, which was described in detail in [29]. As a criterion of the completion of the iterative procedure, we used the condition

$$\left|R_d^{\exp} - R_d^{\mathrm{calc}}\right| \Big/ R_d^{\exp} + \left|T_t^{\exp} - T_t^{\mathrm{calc}}\right| \Big/ T_t^{\exp} < 0.001,$$

where $R_d^{\exp}$, R_d^{calc}, $T_t^{\exp}$, and T_t^{calc} are the experimentally determined and theoretically calculated diffuse reflection and total transmission coefficients.

RESULTS AND DISCUSSION

Figure 1 shows the typical total transmission and diffuse reflection spectra of a sample of sclera recorded on a Cary-2415 spectrophotometer in the spectral range 370–2500 nm. The shape of the presented spectra is mainly determined by the spectral dependence of the scattering coefficient of collagen fibers of sclera and by absorption bands of water of interstitial matrix. It can be seen from Fig. 1 that, in both the visible and IR spectral ranges, the shape of the total transmission spectrum rather well correlates with the shape of the diffuse reflection spectrum, i.e., with increasing wavelength, the diffuse reflection and total transmission coefficients of the biotissue simultaneously increase and decrease showing sharp dips in the range of absorption bands of water.

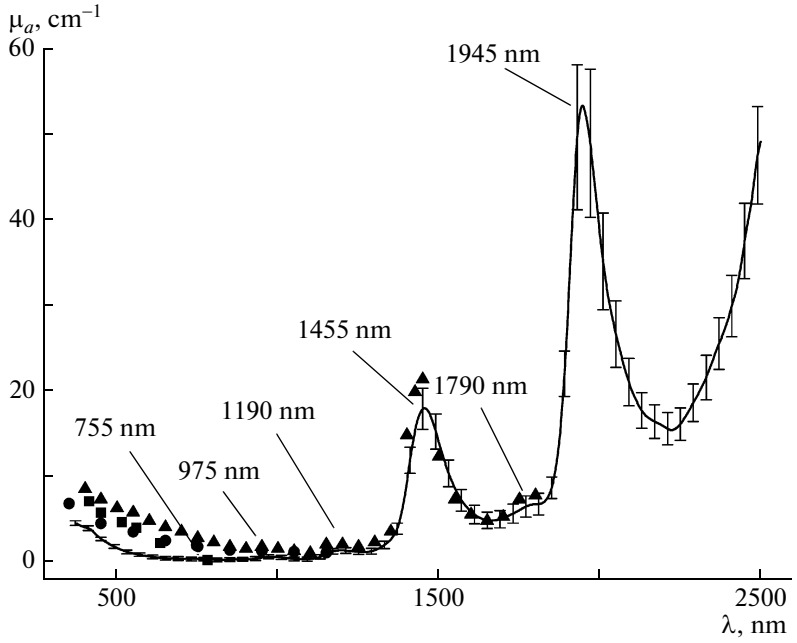

Fig. 2. Spectral dependence of absorption coefficient μ_a of human sclera calculated from experimental data by the IAD method. Vertical lines show standard deviations. Symbols correspond to data from the literature: (●) [6], (■) [7], and (▲) [10].

At present, the absorption spectrum of water has been well studied. In the visible wavelength range, the absorption of water is negligibly small [30]. In the near-IR spectral range, water is the main chromophore, having the absorption bands peaked at 754, 975, 1196, 1455, 1790, and 1930 nm [31, 32]. Figure 1 shows that the dips corresponding to the absorption bands of water are observed both in the total transmission spectrum and in the diffuse reflection spectrum of the sample of the eye sclera tissue.

Figures 2 and 3 present the spectra of absorption and transport scattering coefficient calculated by the IAD method from experimental values of the diffuse reflection and total transmission coefficients. An analysis of the presented absorption and scattering spectra shows that the application of the IAD method for determining the optical parameters of these samples of biotissue is correct. The maximal photon transport free pathlength calculated by the formula $1/(\mu_a + \mu_s')$ and observed at a wavelength of 1300 nm is 0.56 mm. Taking into account the size of the probing beam incident on the surface of the sample of the biotissue (5 × 5 mm), the minimal size of the sample should be at least 7 mm, which is implemented for the smallest of the studied samples, the area of which is about 300 mm^2 and the size of which is 15 × 20 mm.

Figure 2 shows the absorption spectrum of sclera in the spectral range 370–2500 nm. Vertical lines show the values of the standard deviation (SD) calculated by the formula

$$SD = \sqrt{\sum_{i=1}^{N}\left(\bar{\mu}_a - \mu_{ai}\right)^2 \Big/ N(N-1)},$$

where $N = 10$ is the number of measured samples; μ_{ai} is the absorption coefficient of the ith sample of the biotissue; and $\bar{\mu}_a$ is the average absorption coefficient at each spectral point, which is found by the formula $\sum_{i=1}^{N}\mu_{ai}/N$. In the spectrum, one can clearly see the absorption bands of water with maxima at 1190, 1455, 1790, and 1945 nm. The absorption bands of water with maxima at 754 and 975 nm can be poorly observed in the absorption spectrum of sclera because of their low intensity. The observed increase in the absorption in the range above 2200 nm is the short-wavelength shoulder of the absorption band of water with a maximum at 2950 nm. An increase in the standard deviation of the absorption coefficient observed in the range of the absorption bands indicates that different biotissue samples contain different amounts of water.

The symbols in Fig. 2 show the experimental data from the literature [6, 7, 10]. A comparison of our data with those of other authors shows that they agree fairly well with each other, which is especially clearly seen upon comparison of our data with data of [10] in the range 900–1800 nm. In the range 400–900 nm, our data agree somewhat worse with the data of [6, 7, 10], where the optical characteristics of rabbit [6] and pig

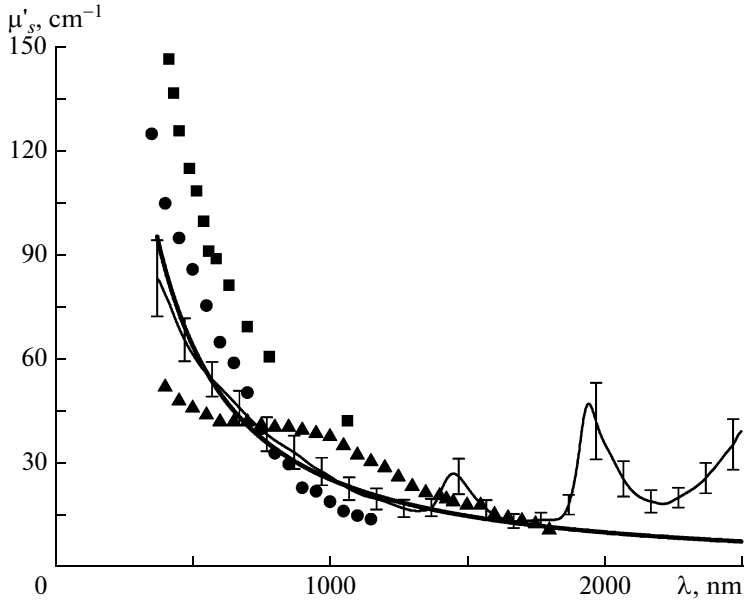

Fig. 3. Spectral dependence of transport scattering coefficient μ_s' of human sclera calculated from experimental data by the IAD method (thin solid curve) and approximation of this dependence by the power function $2.411 \times 10^5\lambda^{-1.325}$ (thick solid curve). Vertical lines show standard deviations. Symbols correspond to data from the literature: (●) [6], (■) [7], and (▲) [10].

sclera [7, 10] were studied, which can be related to the higher pigmentation (the presence of melanin) of sclera of animals than in human sclera.

Figure 3 presents the spectral dependence of the transport scattering coefficient of sclera. This dependence was obtained by averaging of the spectra of the transport scattering coefficient of each of the ten biotissue samples. Vertical lines show the standard deviations of the scattering characteristics of sclera obtained during the measurements. It can be clearly seen that, in the range 370–1300 nm, the transport scattering coefficient rather smoothly (monotonically) decreases in the direction of longer wavelengths, which, on the whole, corresponds to the general character of the spectral behavior of scattering characteristics of biotissues [4, 33–35]. However, beginning at 1300 nm, the transport scattering coefficient increases with increasing wavelength and a distortion of the shape of the scattering spectrum is observed, i.e., a nonmonotonic behavior of the spectrum in the range of absorption bands. Symbols in Fig. 3 show experimental data from the literature [6, 7, 10]. It can be seen from the figure that our data agree quite well with the data of other authors.

In the visible and near-IR ranges, the spectral dependence of the transport scattering coefficient is approximated with a good accuracy by a power function $\mu_s'(\lambda) = a\lambda^{-w}$ [33–35], where the parameter a is determined by the concentration of scattering centers of the biotissue and the ratio of the refractive indices of scatterers and the surrounding medium, while the parameter w (the wave exponent) characterizes the average size of scatterers and determines the spectral behavior of the transport scattering coefficient [36–38]. Figure 3 shows the approximation of the spectrum of the transport scattering coefficient by the function $\mu_s'(\lambda) = 2.411\times10^5\lambda^{-1.325}$, where λ is the wavelength (in nm). It can be seen from this figure that this function well approximates the experimental data in the range 400–1300 nm, whereas, in the spectral range 1300–2500 nm, a considerable discrepancy is observed between the experimental data and the approximating dependence.

Typically, for tissues of aorta, skin, dura mater, etc., the wave exponent is 1–2 [18, 34, 35, 39–43]. In this case, the size of scatterers lie in the range 0.1–1 μm. The wave exponent of 1.325 that we obtained is indicative of the occurrence of rather large scatterers in the sclera, such as bundles of collagen fibers and their plexuses. Assuming that the refractive index of collagen fibers of the sclera is 1.47 and that of interstitial fluid is 1.36 [4], and applying the method proposed in [44], we can estimate the average size of scatterers in the sclera to be 0.5 ± 0.05 μm, which is rather consistent with the structural and morphological peculiarities of this biotissue. Electron microscopy shows that elementary scatterers in sclera are thin collagen fibers, which have sizes in the range 30–300 nm and average diameters of about 133 nm, and are packed into ribbon bundles with a thickness of 0.5–6 μm and with width of 1–50 μm [45]. The data of atomic force microscopy show that the average size of collagen fibers is 310.5 nm with a spread of 118–1268 nm [46]. Therefore, the value of 0.5 ± 0.05 μm that we found for the

average diameter of scatterers agrees quite well with data of electron and atomic force microscopy.

The deviation of the spectrum of the transport scattering coefficient in the range of absorption bands from the monotonic dependence can be explained by an increase in the effect of the imaginary part of the complex refractive index of scattering centers, the role of which is, in this case, played by collagen fibers. According to the Mie theory [47], the intensity of scattered radiation is mainly determined by the complex refractive index of scatterers of biotissue and the increase in the imaginary part of the complex refractive index in the range of the absorption bands leads to a change in the scattering cross section and, naturally, to a change in the transport scattering coefficient in this spectral range. In addition, an increase in the imaginary part of the complex refractive index of scatterers causes a considerable decrease in the scattering anisotropy factor g, which, on par with the scattering coefficient of biotissue μ_s, forms the spectrum of the transport scattering coefficient $\mu_s' = \mu_s(1 - g)$. In [48–50], it was experimentally shown that, in the range of the water absorption bands at 1450 and 1930 nm, a decrease in both μ_s and g is observed, which inevitably leads to an increase in the transport scattering coefficient and to the appearance of bands in its spectrum. In this case, the magnitude of the decrease in the scattering anisotropy factor in the range of the absorption bands is proportional to the intensity of the absorption bands. These measurements are consistent with the data in [51, 52], where a theory was developed and a computer model was constructed to explain the observed behavior of the spectrum of the transport scattering coefficient. The data presented in Fig. 3 are consistent with those presented above. In the range of 370–1300 nm, the absorption of water is either insignificant or absorption bands are comparatively weak (Fig. 2). Correspondingly, the scattering spectrum in this spectral range is mainly formed by the real part of the complex refractive index, and the spectrum of the transport scattering coefficient rather monotonically decreases in the direction of longer wavelengths. In the range of 1300–2500 nm, the absorption spectrum of the sclera exhibits rather intense absorption bands of water. The occurrence of strong absorption bands results in that the formation of the scattering spectrum is affected by not only the real, but also the imaginary, part of the complex refractive index of scattering centers of biotissue, which manifests itself as an increase in the transport scattering coefficient in this spectral range with rather strong peaks in the range of absorption bands.

Because, structurally, the sclera is a typical representative of fibrous tissues, we compared the optical characteristics of sclera and bloodless skin dermis, which, structurally, also refers to fibrous tissues [4], since both these tissues are mainly formed by large bundles of collagen fibers that are arranged parallel to the biotissue surface and do not contain any large blood vessels, marked lipid inclusions, or other components. The water contents in these tissues are also comparable. Thus, the volume fraction of water in the skin dermis is estimated to be 70% [5], 75% [53], 65% [54], and 65.1–75.8% [55], which, on average, yields $70.2 \pm 5.2\%$. In turn, the water contents in the sclera are estimated to be 77.7% [56], $71.3 \pm 3.9\%$ [57], and 68% [58], which, on average, yields $72.3 \pm 4.9\%$. The refractive indices of these biotissues are also close to each other. In [58], it was shown that the refractive index of human sclera (at a wavelength of 589 nm) is 1.385 ± 0.005. According to [59], the refractive index of human skin dermis at this wavelength is 1.388. This compliance allows us to assume that the volume fractions of scattering particles in sclera and human skin dermis are also the same (or close), which is supported by the data of [60, 61], where it was shown that the volume fractions of scatterers in these biotissues are 21%.

Figures 4 and 5 show the spectra of absorption and transport scattering coefficient of sclera measured in this work. Furthermore, these spectra are also compared with the optical parameters of human and animal skin dermis available in the literature. Figure 4 shows the absorption spectrum of sclera in the spectral range 370–2500 nm measured in this work and presented in Fig. 2. The symbols in Fig. 4 show the experimental data from the literature [5, 10, 18, 49, 62–64]. The comparison of the absorption spectrum of sclera that we measured and absorption spectra of bloodless skin dermis obtained by other authors shows rather good agreement between them. In the visible spectral range, the best agreement is observed between the absorption of sclera and the data of [18, 62]. In the near-IR range of 800–1300 nm, the absorption spectrum of sclera is in excellent agreement with absorption coefficients obtained in [5, 18, 49, 64]. In the range of 1300–1800 nm, the absorption spectrum of sclera agrees well with the absorption spectra of dermis from [5, 10, 49, 64].

Figure 5 compares the spectra of the transport scattering coefficient for sclera (Fig. 3) and for dermis from [5, 10, 18, 49, 62–64]. The comparison shows quite good agreement between them despite the relatively large scatter of values of the transport scattering coefficient of dermis, especially, in the visible wavelength range. In this range, the best agreement is observed between the scattering in sclera and the data of [64]. Somewhat worse agreement is observed in the near-IR range 800–1300 nm, where the scattering coefficients of sclera somewhat exceed scattering coefficients of skin dermis obtained in [5, 10, 18, 62, 64]. In the range of 1300–1600 nm, the scattering spectrum of sclera is consistent with the scattering spectra of the dermis presented in [49, 64]. Finally, in the range of 1600–1800 nm, the spectrum of the transport scattering coefficient of sclera agrees well with the spectrum of the transport scattering coefficient of dermis obtained in [18].

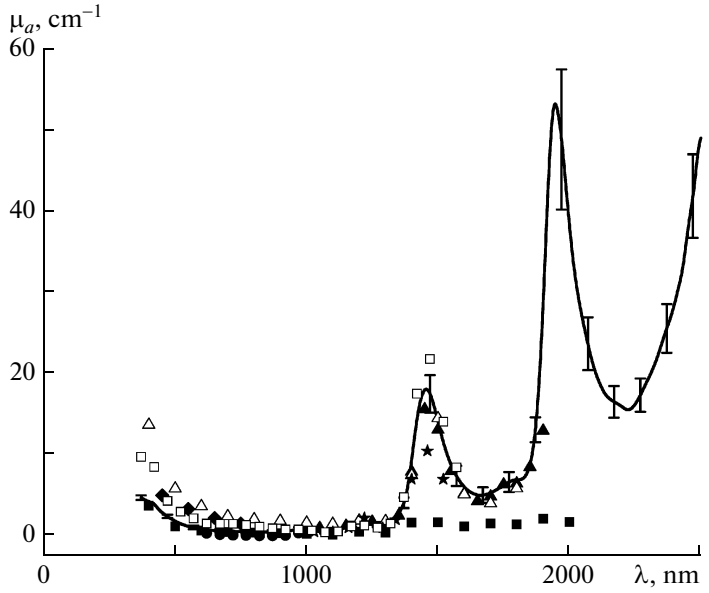

Fig. 4. Spectral dependences of absorption coefficients μ_a of sclera and bloodless skin dermis. Vertical lines show standard deviations. Symbols correspond to absorption spectrum of skin dermis: (▲) [5], (△) [10], (■) [18], (★) [49], (●) [62], (◆) [63], and (□) [64].

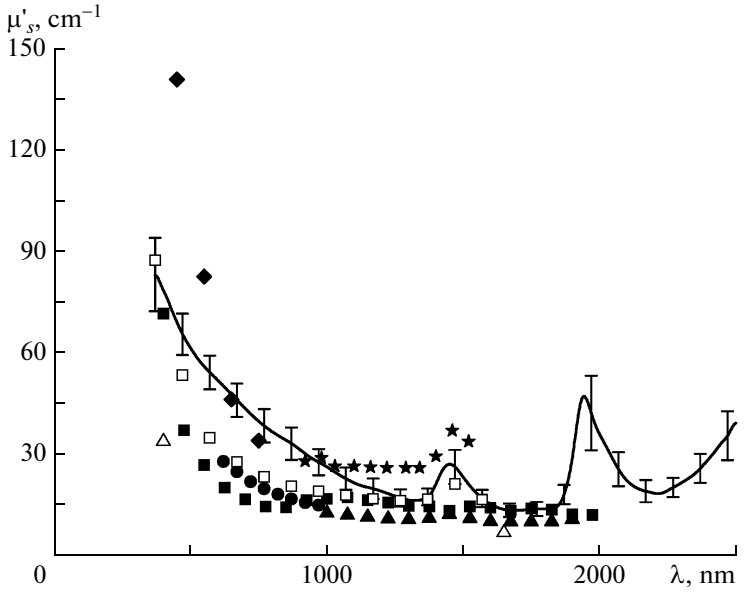

Fig. 5. Spectral dependences of transport scattering coefficients μ'_s of human sclera and bloodless skin dermis. Vertical lines show standard deviations. Symbols correspond to spectrum of transport scattering coefficient of skin dermis: (▲) [5], (△) [10], (■) [18], (★) [49], (●) [62], (◆) [63], and (□) [64].

Therefore, overall, we can conclude that the comparison of the optical characteristics of sclera and bloodless skin dermis makes it possible to confirm the statement made above on the structural similarity of these biotissues and the similarity of their optical characteristics despite certain distinctions (Figs. 4, 5). At the same time, upon the construction of an optical model of fibrous tissues, it is also necessary to take into account certain differences in the structure of these biotissues. Thus, in addition to collagen fibers, which is the main protein of sclera, bloodless skin dermis also contains elastin fibers, which differ in the size and

degree of hydration from collagen fibers. In addition, it is also necessary to take into account the greater dispersivity of scatterers in skin dermis. As opposed to sclera, the size of fiber bundles in skin dermis is 1–8 μm [15] with a maximum at 2.8 μm [60], which is apparently one of the reasons for the difference between the scattering characteristics of sclera and skin dermis. It is also possible that the refractive indices of direct scatterers in these tissues are different, which may be related to the different contents of proteoglycans and glycosaminoglycans in the interstitial matrix and, as a consequence; to differences in the proportional content of free and bound water in biotissues; and, correspondingly, to different hydration of proteins [65].

CONCLUSIONS

The development of optical methods of diagnostics and therapy of ophthalmological diseases require the knowledge of optical characteristics of sclera in a wide wavelength range. In this work, we experimentally studied the optical parameters of sclera and compared them with the known data from the literature. Experiments were performed in vitro on a Cary-2415 spectrophotometer in the spectral range of 370–2500 nm. Based on the experimentally determined diffuse reflection and total transmission spectra, we calculated the spectra of the absorption and transport scattering coefficient using the IAD method. The results obtained in this work can be used in the development of new optical methods of diagnostics and therapy of eye diseases, as well as in optimization of already existing methods.

ACKNOWLEDGMENTS

We are grateful to T.G. Kamenskikh (Department of Eye Diseases at the Saratov State Medical University) for providing samples of sclera and consultations. This work was supported by the Russian Foundation for Basic Research (project no. 08-02-92224) and the US Civilian Research and Development Foundation (grant no. RUB 1-2932-SR-08).

REFERENCES

1. V. V. Tuchin, Usp. Fiz. Nauk **167** (5), 517 (1997).
2. *Optical Biomedical Diagnostics*, Ed. V. V. Tuchin (Fizmatlit, Moscow, 2007) [in Russian].
3. D. A. Zimnyakov and V. V. Tuchin, Kvantovaya Élektron. (Moscow) **32** (10), 849 (2002).
4. V. V. Tuchin *Tissue Optics: Light Scattering Methods and Instruments for Medical Diagnosis* (SPIE Press, Bellingham, 2007), 882 p.
5. T. L. Troy and S. N. Thennadil, J. Biomed. Opt. **6** (2), 167 (2001).
6. B. Nemati, H. G. Rylander III, and A. J. Welch, Appl. Opt. **35** (19), 3321 (1996).
7. M. Hammer, A. Roggan, D. Schweitzer, and G. Muller, Phys. Med. Biol. **40**, 963 (1995).
8. A. Vogel, C. Dlugos, R. Nuffer, and R. Birngruber, Las. Surg. Med. **11**, 331 (1991).
9. I. Fine, E. Loewinger, A. Weinreb, and D. Weinberger, Phys. Med. Biol. **30** (6), 565 (1985).
10. E. K. Chan, B. Sorg, D. Protsenko, M. O'Neil, M. Motamedi, and A. J. Welch, IEEE J. Sel. Top. Quant. Electron. **2** (4), 943 (1996).
11. S. A. Prahl, M. J. C. van Gemert, and A. J. Welch, Appl. Opt. **32** (4), 559 (1993).
12. J. F. Beek, P. Blokland, P. Posthumus, M. Aalders, J. W. Pickering, H. J. C. M. Sterenborg, and M. J. C. van Gemert, Phys. Med. Biol. **42**, 2255 (1997).
13. S. C. Gebhart, W.-C. Lin, and A. Mahadevan-Jansen, Phys. Med. Biol. **51**, 2011 (2006).
14. J. Qu, C. MacAulay, S. Lam, and B. Palcic, Appl. Opt. **33** (31), 7397 (1994).
15. I. S. Saidi, S. L. Jacques, and F. K. Tittel, Appl. Opt. **34** (31), 7410 (1995).
16. D. K. Sardar, M. L. Mayo, and R. D. Glickman, J. Biomed. Opt. **6** (4), 404 (2001).
17. D. K. Sardar, R. M. Yow, A. T. C. Tsin, and R. Sardar, J. Biomed. Opt. **10** (5), 051 501 (2005).
18. A. N. Bashkatov, E. A. Genina, V. I. Kochubey, and V. V. Tuchin, Appl. Phys. D **38**, 2543 (2005).
19. A. N. Bashkatov, É. A. Genina, V. I. Kochubeĭ, V. V. Tuchin, E. É. Chikina, A. B. Knyazev, and O. V. Mareev, Opt. Spektrosk. **97** (6), 1043 (2004) [Opt. Spectrosc. **97** (6), 978 (2004)].
20. A. N. Bashkatov, É. A. Genina, V. I. Kochubeĭ, and V. V. Tuchin, Opt. Spektrosk. **99** (5), 868 (2005) [Opt. Spectrosc. **99** (5), 836 (2005)].
21. T. J. Farrell, M. S. Patterson, and B. C. Wilson, Med. Phys. **19**, 879 (1992).
22. J. S. Dam, P. E. Andersen, T. Dalgaard, and P. E. Fabricius, Appl. Opt. **37** (4), 772 (1998).
23. F. Bevilacqua, D. Piguet, P. Marquet, J. D. Gross, B. J. Tromberg, and C. Depeursinge, Appl. Opt. **38** (22), 4939 (1999).
24. D. W. Ebert, C. Roberts, S. K. Farrar, W. M. Johnston, A. S. Litsky, and A. L. Bertone, J. Biomed. Opt. **3** (3), 326 (1998).
25. S. K. Farrar, C. Roberts, W. M. Johnston, and P. A. Weber, Laser Surg. Med. **25**, 348 (1999).
26. W. E. Vargas, J. Opt. A **4**, 452 (2002).
27. J. W. Pickering, S. A. Prahl, Wieringen. N. van, J. F. Beek, H. J. C. M. Sterenborg, and M. J. C. van Gemert, Appl. Opt. **32** (4), 399 (1993).
28. S. A. Prahl, in *Optical–Thermal Response of Laser-Irradiated Tissue*, Ed. by A J. Welch and M. J. C. van Gemert (Plenum, New York, 1995), p. 101.
29. B. D. Bunday, *Basic Optimization Methods* (Edward Arnold, London, 1984; Radio i Svyaz', Moscow, 1988).
30. R. C. Smith and K. S. Baker, Appl. Opt. **20**, 177 (1981).
31. L. Kou, D. Labrie, and P. Chylek, Appl. Opt. **32**, 3531 (1993).
32. K. F. Palmer and D. Williams, J. Opt. Soc. Am. **64**, 1107 (1974).

33. J. R. Mourant, T. Fuselier, J. Boyer, T. M. Johnson, and I. J. Bigio, Appl. Opt. **36** (4), 949 (1997).
34. J. M. Schmitt and G. Kumar, Appl. Opt. **37** (13), 2788 (1998).
35. R. K. Wang, J. Mod. Opt. **47** (1), 103 (2000).
36. S. Yu. Shchegolev and V. I. Klenin, Opt. Spektrosk. **31** (5), 794 (1971).
37. N. G. Khlebtsov, A. G. Mel'nikov, and S. Yu. Shchegolev, Kolloidn. Zh. **53** (5), 928 (1991).
38. N. G. Khlebtsov and A. G. Mel'nikov, Zh. Prikl. Spektrosk. **56** (3), 435 (1992).
39. R. M. P. Doornbos, R. Lang, M. C. Aalders, F. W. Cross, and H. J. C. M. Sterenborg, Phys. Med. Biol. **44**, 967 (1999).
40. I. F. Cilesiz and A. J. Welch, Appl. Opt. **32** (4), 477 (1993).
41. W.-C. Lin, M. Motamedi, and A. J. Welch, Appl. Opt. **35** (19), 3413 (1996).
42. G. Vargas, E. K. Chan, J. K. Barton, H. G. Rylander III, and A. J. Welch, Las. Surg. Med. **24**, 133 (1999).
43. N. Ghosh, S. K. Mohanty, S. K. Majumder, and P. K. Gupta, Appl. Opt. **40**, 176 (2001).
44. V. I. Klenin, S. Yu. Shchegolev, and V. I. Lavrushin, *Characteristic Functions of Light Scattering by Dispersed Systems* (Sarat. Gos. Univ., Saratov, 1977) [in Russian].
45. Y. Komai and T. Ushiki, Invest. Ophth. Vis. Sci. **32**, 2244 (1991).
46. D. Meller, K. Peters, and K. Meller, Cell. Tissue Res. **288**, 111 (1997).
47. C. R. Bohren and D. R. Huffman *Absorption and Scattering of Light by Small Particles* (Wiley, New York 1983; Mir, Moscow, 1986).
48. J.-P. Ritz, A. Roggan, C. Isbert, G. Muller, H. Buhr, and C.-T. Germer, Las. Surg. Med. **29**, 205 (2001).
49. Y. Du, X. H. Hu, M. Cariveau, G. W. Kalmus, and J. Q. Lu, Phys. Med. Biol. **46**, 167 (2001).
50. A. N. Bashkatov, E. A. Genina, V. I. Kochubey, A. A. Gavrilova, S. V. Kapralov, V. A. Grishaev, and V. V. Tuchin, Med. Las. Appl. **22**, 95 (2007).
51. Q. Fu and W. Sun, Appl. Opt. **40** (9), 1354 (2001).
52. W. Sun, N. G. Loeb, and B. Lin, Appl. Opt. **44** (12), 2338 (2005).
53. G. Altshuler, M. Smirnov, and I. Yaroslavsky, J. Phys. D **38**, 2732 (2005).
54. S. L. Jacques, J. Biophotonics. **3** (1–2), 75 (2010).
55. R. F. Reinoso, B. A. Telfer, and M. Rowland, J. Pharmacol. Toxicol. Meth. **38**, 87 (1997).
56. A. Edwards and M. R. Prausnitz, AIChE J. **44** (1), 214 (1998).
57. O. A. Boubriak, J. P. G. Urban, S. Akhtar, K. M. Meek, and A. J. Bron, Exp. Eye Res. **71**, 503 (2000).
58. P. O. Rol, PhD Thesis (Swiss Federal Instit. Technol., Zurich, 1992).
59. H. Ding, J. Q. Lu, W. A. Wooden, P. J. Kragel, and X.-H. Hu, Phys. Med. Biol. **51**, 1479 (2006).
60. S. Jacques, OSA TOPS Adv. Opt. Imag. Photon Migr. **2**, 364 (1996).
61. D. B. Ameen, M. F. Bishop, and T. McMullen, Biophys. J. **75**, 2520 (1998).
62. C. R. Simpson, M. Kohl, M. Essenpreis, and M. Cope, Phys. Med. Biol. **43**, 2465 (1998).
63. S. A. Prahl, PhD Thesis, (Texas Univ., Austin, 1988).
64. E. Salomatina, B. Jiang, J. Novak, and A. N. Yaroslavsky, J. Biomed. Opt. **11** (6), 064 026 (2006).
65. S. H. Chung, A. E. Cerussi, C. Klifa, H. M. Baek, O. Birgul, G. Gulsen, S. I. Merritt, D. Hsiang, and B. J. Tromberg, Phys. Med. Biol. **53**, 6713 (2008).

Translated by V. Rogovoi